

## Article

# Refractivity of $P_2O_5$ - $Al_2O_3$ - $SiO_2$ Glass in Optical Fibers

Mikhail E. Likhachev <sup>1,\*</sup>, Tatiana S. Zaushitsyna <sup>1</sup>, Vitaliya A. Agakhanova <sup>1</sup>, Liudmila D. Iskhakova <sup>1</sup>, Svetlana S. Aleshkina <sup>1</sup> , Mikhail M. Bubnov <sup>1</sup>, Alexey S. Lobanov <sup>2</sup>  and Denis S. Lipatov <sup>2</sup>

<sup>1</sup> Prokhorov General Physics Institute of the Russian Academy of Sciences, Dianov Fiber Optics Research Center of the Russian Academy of Sciences, 119991 Moscow, Russia; vita@fo.gpi.ru (V.A.A.); ldisk@fo.gpi.ru (L.D.I.); sv\_alesh@fo.gpi.ru (S.S.A.); bubnov@fo.gpi.ru (M.M.B.)

<sup>2</sup> G.G. Devyatykh Institute of Chemistry of High-Purity Substances, Russian Academy of Sciences, 49 Tropinin St., 603951 Nizhny Novgorod, Russia; lobanov@ihps-nnov.ru (A.S.L.); lipatov@ihps-nnov.ru (D.S.L.)

\* Correspondence: likhachev@fo.gpi.ru

**Abstract:** A significant change in the refractive index profiles for the large mode area phosphoroaluminosilicate (PAS) core optical fibers was observed in comparison to that in preforms. This study shows that the refractive index of the PAS core can vary from negative (in preform) to positive (in fiber), and the difference in the refractive index between the core and preform can exceed a few thousand. By measuring a large set of fibers with different concentrations of  $P_2O_5$  and  $Al_2O_3$ , we define the refractivity of each dopant ( $P_2O_5$ ,  $Al_2O_3$  and  $AlPO_4$  joint) after drawing fiber from the preform and discuss the possible origin of the observed refractive index variation.

**Keywords:** large mode area fibers; refractive index; phosphorosilicate glass; aluminosilicate glass; phosphoroaluminosilicate glass



**Citation:** Likhachev, M.E.; Zaushitsyna, T.S.; Agakhanova, V.A.; Iskhakova, L.D.; Aleshkina, S.S.; Bubnov, M.M.; Lobanov, A.S.; Lipatov, D.S. Refractivity of  $P_2O_5$ - $Al_2O_3$ - $SiO_2$  Glass in Optical Fibers. *Photonics* **2023**, *10*, 1383. <https://doi.org/10.3390/photonics10121383>

Received: 22 November 2023

Revised: 7 December 2023

Accepted: 13 December 2023

Published: 15 December 2023



**Copyright:** © 2023 by the authors. Licensee MDPI, Basel, Switzerland. This article is an open access article distributed under the terms and conditions of the Creative Commons Attribution (CC BY) license (<https://creativecommons.org/licenses/by/4.0/>).

## 1. Introduction

Phosphoroaluminosilicate (PAS) glass has unique properties, which make it most promising for utilization in large-mode-area (LMA) optical fibers. First, there is the low refractivity of PAS glass near the equimolar concentration of  $P_2O_5$  and  $Al_2O_3$  [1–3] caused by the formation of the  $AlPO_4$  joint [3]. Second is the high solubility of rare earth ions [4,5], despite the similarity of the PAS glass network and undoped silica glass. Third is its low sensitivity to the photodarkening effect in the case of Yb-doped fibers [5–8]. These features have made PAS glass the gold standard for the fabrication of large-mode-area fibers doped with rare-earth elements [9–13].

Typically, the design of LMA fibers is a balance between bend sensitivity and operation with diffraction-limited beam quality [14], which requires exact knowledge and precise control of the refractive index of the fiber core. There are few works where the refractivity of PAS glass relative to its compound is studied in detail [1,2,15,16]. However, the refractive index profile (RIP) in these studies was measured in preforms of optical fibers and not in the optical fibers drawn from them. Such an approach is widespread due to the large core size in the preform, and it is possible to measure RIP and concentration distribution with a high accuracy. Typically, for binary glasses (for example,  $SiO_2$ - $GeO_2$ ,  $SiO_2$ - $P_2O_5$ ,  $SiO_2$ - $Al_2O_3$ ,  $SiO_2$ -F and others), additional factors, such as stress frozen into glass due to a difference in the thermal expansion coefficient, do not affect measurements noticeably as the refractive index difference between the core and the cladding grow much faster due to dopant refractivity than other factors.

However, the measurements of RIP in the fiber preformed for estimation RIP in optical fiber become questionable for PAS glasses near the equimolar concentration of  $P_2O_5$  and  $Al_2O_3$ . Indeed, despite a high concentration of both dopants, the refractive index difference between the core and the cladding could be nearly zero in such glasses. Thus, factors that were previously considered negligible (i.e., internal core stress, drawing condition, etc.)

might affect the refractive index considerably. Small index changes become critically important in the case of LMA fibers because the target refractive index difference could be as low as 0.0013 for standard step-index fibers [17] or even nearly zero (in the case of photonics bandgap and photonics crystal fibers) [11].

The aim of our work was to study the refractivity of PAS glass directly in optical fibers and reveal any difference compared to the measurements of preforms. In the current communication, we show a significant discrepancy between the RIP in preforms and the optical fibers drawn from it. Also, we define exact formulas that describe the influence of the doping level of  $\text{Al}_2\text{O}_3$  and  $\text{P}_2\text{O}_5$  on the refractive index difference between the doped core and undoped silica glass cladding.

## 2. Materials and Methods

To perform the current study, we fabricated a series of fiber preforms using the conventional method of modified chemical vapor deposition (MCVD). All the dopants were deposited from the gas phase. For this aim, we used the low-boiling liquids  $\text{SiCl}_4$ ,  $\text{GeCl}_4$ ,  $\text{POCl}_3$  and  $\text{C}_2\text{F}_3\text{Cl}_3$  as a precursor. As a precursor for doping with  $\text{Al}_2\text{O}_3$ , we used  $\text{AlCl}_3$  (99.999% purity on metals basis). On the contrary to other precursors,  $\text{AlCl}_3$  is a low-volatile solid under ordinary conditions, and to achieve a high enough vapor pressure, it is necessary to heat it up to 125–140 °C. Moreover, in normal conditions,  $\text{AlCl}_3$  can react with  $\text{POCl}_3$  and form complex compounds. For this reason, the MCVD set-up was equipped with a system for the evaporation of solid precursors and vapor delivery.  $\text{AlCl}_3$  powder was installed into the container and stabilized at a temperature of 130 °C. The vapor of  $\text{AlCl}_3$ , together with the carrier gas Ar, was delivered to the reaction zone through the heated lines until it mixed with other components in the supporting tube. In all other parameter methods, the fabrication of preforms was similar to the standard MCVD process. The RIP in each preform was measured using a Photon Kinetics preform analyzer PK2600. Each preform was measured at a few positions along its axis to confirm uniformity. At each position, measurements were performed for three rotation angles around the preform axis before it was averaged.

The fabricated preform was drawn into optical fibers with a core diameter of 20–30  $\mu\text{m}$  and outer diameter of 125  $\mu\text{m}$ . A relatively large core diameter was chosen to exclude the influence of dopant diffusion on the results of the measurements. Special attention was paid to the optical fibers' drawing condition. It is known that drawing tension could noticeably affect the refractive index difference between the core and cladding [18]—the refractive index of undoped silica cladding is reduced with the growth of drawing tension, and the difference may reach 0.0014 when the drawing tension exceeds 300 g. Such an index change is larger than the target core-cladding index difference in some types of optical fibers (those where target core NA = 0.062 [17]) and could result in a significant variation in fiber parameters along the length (due to the variation in drawing tension, which is not always possible to precisely control during fiber drawing). To avoid this effect, all the fibers in our study were drawn with a tension below 30 g. It presents the variation in the refractive index of the undoped silica cladding as less than 0.00014, which is acceptable for our study as it is on the level of measurement inaccuracy for our equipment.

The spatial distribution of chemical elements was determined in the fiber samples with the help of energy-dispersive X-ray spectroscopy (EDXS) (AZtecENERGY analytical systems; Oxford Instruments, Oxfordshire, UK; JSM5910-LV, JEOL, Tokyo, Japan). The analyses were performed in the fiber samples via scanning along the core diameter of the studied samples. To calibrate our setup, we used an etalon based on the  $\text{AlPO}_4$  single crystal for the calibration of the signal corresponding to P and Al atoms. It allowed us to achieve the highest accuracy of measurements due to the similarity of the etalon and the studied glass compounds.

RIPs in the fabricated fibers were measured using the fiber analyzer EXFO NR9200HR. In this case, two scans were made in the orthogonal axes, and then four half profiles were averaged to achieve the distribution of the refractive index along the fiber radius.

Both distributions (refractive index profile and compound) were measured with a high resolution (better than 1  $\mu\text{m}$ ), which allowed us to compare the refractive index and glass content along all radius positions (in some fibers, we used not one position, but two or even three different radius positions). To reduce the measurement error caused by the possible non-circularity of the fiber, we used those sections of the fiber cross-section along the radius to collect data, where the refractive index and compound changed most slowly.

### 3. Results

Through a comparison of refractive index profiles measured in optical fibers, a noticeable change in the refractive index of PAS fibers was revealed—the core refractive index became higher compared to that in the optical preforms, and this difference could reach 0.002 for highly  $\text{P}_2\text{O}_5$ - and  $\text{Al}_2\text{O}_3$ -doped fibers. The most noticeable change was observed in optical fibers with a refractive index difference close to zero. The most remarkable example—the change in the refractive index difference between the core and the cladding from negative to positive—was observed in fiber PAS#1 (see Figure 1a), doped with 4.6 mol.% of  $\text{P}_2\text{O}_5$  and 4.2 mol.% of  $\text{Al}_2\text{O}_3$ . The observed behavior was completely different from that in germanosilicate fibers, where almost no change in RIP between the fiber and preform was observed. As an example, the RIP in the preform GeF, doped with 3 mol.% of  $\text{GeO}_2$  and 2.7 mol.% of F, is shown in Figure 1b together with the RIP measured in fiber drawn from this preform.

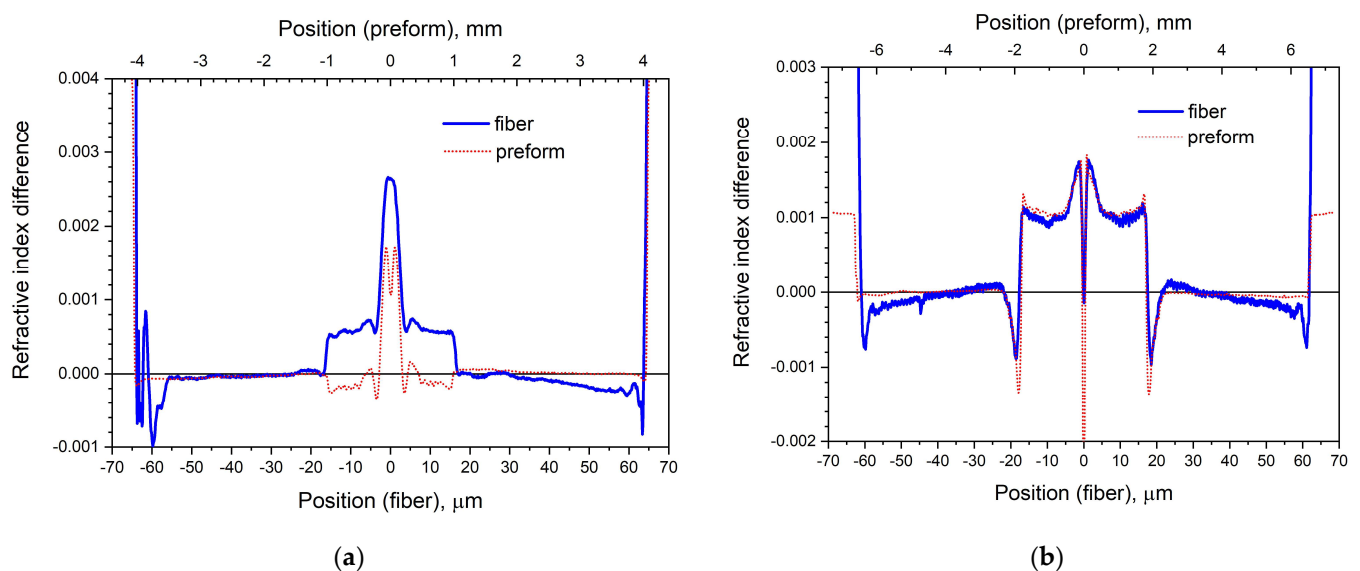


**Figure 1.** (a) Refractive index profile measured in the preform PAS#1 (dashed curve) and in the fiber drawn from the same preform (solid curve); (b) refractive index profile measured in the preform GeF (dashed curve) and in the fiber drawn from the same preform.

Even more importantly, in the preform with the distribution of non-uniform dopants along the core radius, the change in the refractive index was also non-uniform. This feature could change the final shape of the RIP critically. An example is presented in Figure 2, where the RIPs and measured dopant distribution for fiber PAS#2 are shown. Despite the quite similar distribution of  $\text{P}_2\text{O}_5$  and  $\text{Al}_2\text{O}_3$  along the radius, the RIP was extremely sensitive to the variation in relative concentrations of these dopants. This feature is well known for PAS glasses [1–3,15]. The effect is caused by the formation of the  $\text{AlPO}_4$  joint in PAS glass—almost all Al and P atoms are structurally bonded in  $\text{AlPO}_4$ . Only an excess amount of these dopants stays in its ordinary form ( $\text{P}_2\text{O}_5$  for PAS glass with an excess of phosphorous and  $\text{Al}_2\text{O}_3$  for PAS glass with an excess of aluminum). The crystals  $\text{AlPO}_4$  and  $\text{SiO}_2$  have almost identical parameters (alpha-quartz and berlinite). Therefore, quartz and aluminophosphosilicate (with equal amounts of Al and P atoms) glasses have the same

network structure, and, as a consequence, they also have a number of similar properties (including the refractive index). Thus, it is this difference between the concentration of Al and P atoms that defines the RIP. It should be noted that in this paper, we discuss the formal concentration of dopants ( $P_2O_5$  and  $Al_2O_3$ ) in molar %, which is calculated without taking into account the formation of the  $AlPO_4$  joint. This was conducted for reasons of convenience, as the usage of these formal concentrations allows one to easily estimate the concentration of the dopant in excess (by simple subtraction of smaller concentration from the larger one), as well as the concentration of the  $AlPO_4$  joint by doubling the smallest dopant concentration (due to reaction  $P_2O_5 + Al_2O_3 = 2 AlPO_4$ ).

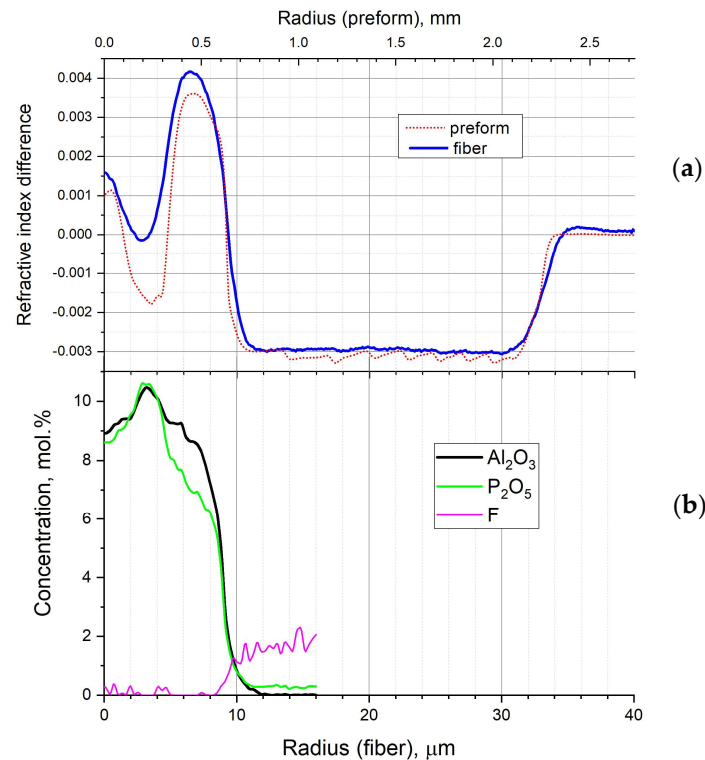


**Figure 2.** (a): Refractive index profile measured in the preform PAS#2 (dashed curve) and in the fiber drawn from the same preform (solid curve); (b): the measured concentration of dopants in the fiber PAS#2.

As can be seen in Figure 2, the molar concentration of  $P_2O_5$  and  $Al_2O_3$  is nearly equal for the radii from 2 μm to 4.5 μm, which coincides with part of the cross-section where the core refractive index in the preform has the minimum value (from  $-0.0018$  to  $-0.0015$  relative to undoped silica layer). This result is in good agreement with the previously reported refractivity of the  $AlPO_4$  joint—as we could estimate its concentration as  $\sim 20$  mol.%—which corresponds to the refractive index difference with undoped silica glass on the level of  $-0.002$  [1,4].

More importantly, the refractive index of the above-mentioned area in the fiber cross-section (radii from 2 μm to 4.5 μm) changes its refractive index by approximately 0.0015 and becomes equal to that of pure silica glass within the accuracy of the measurements. For other regions of the core, the change in the refractive index of the core is much less visible—for regions of the cross-section near radii 0 μm and 6.5 μm, the refractive index changed by only 0.0005 (which is three times smaller compared to the region with an equal atomic content of Al and P).

It is worth noting that preform PAS#2 has a large amount of F-doped cladding, and its refractive index has not changed. This is clear confirmation that the observed effects of refractive index change are related to the properties of PAS glass and not to the drawing condition. Indeed, drawing with high tension results in a change in the refractive index

of undoped silica cladding relative to the whole doped structure [18], and a change in the refractive index of the doped central part and undoped silica cladding is typically constant in this case (though the form of the doped part does not change). In Figure 2, it can be seen that the refractive index difference between F-doped cladding and pure silica cladding is nearly the same as the optical fiber and preform. This means that drawing tension does not affect the refractive index profile in this case.

To quantitatively analyze the behavior of the refractive index of PAS glass, we made the following three sets of preforms: with an aluminosilicate core, a phosphorosilicate core and preforms, the core of which was doped simultaneously with P and Al. The concentration of Al and P varied in a wide range (from 2 mol.% up to 22 mol.% of  $\text{Al}_2\text{O}_3$  and 15 mol.% of  $\text{P}_2\text{O}_5$ ). The first two sets of the preform were used to analyze the refractivity of  $\text{P}_2\text{O}_5$  and  $\text{Al}_2\text{O}_3$  in optical fiber for the cases of binary glasses (phosphorosilicate and aluminosilicate). The obtained results are presented in Figure 3, where the refractive index difference between the doped silica glass and undoped silica glass ( $\Delta n$ ) is shown as a function of the molar concentration of the dopant. It can be seen that, in both cases, dependence is linear and can be described using the following formulas:

$$\Delta n = 0.9 \times 10^{-3} \cdot C(\text{P}_2\text{O}_5) \quad (1)$$

$$\Delta n = 2.2 \times 10^{-3} \cdot C(\text{Al}_2\text{O}_3) \quad (2)$$

where  $C(\text{P}_2\text{O}_5)$  and  $C(\text{Al}_2\text{O}_3)$  are the concentration of  $\text{P}_2\text{O}_5$  and  $\text{Al}_2\text{O}_3$  in molar percentages; Equation (1) corresponds to phosphorosilicate glass, and Equation (2) corresponds to the aluminosilicate glass.

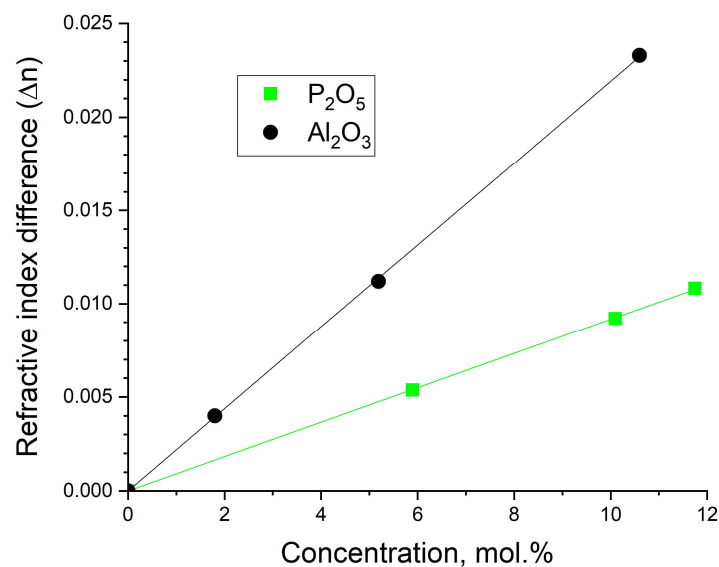


**Figure 3.** Dependence of refractive index difference between core and undoped silica glass cladding on dopant concentration for phosphorosilicate and aluminosilicate fibers.

The obtained dependences of optical fibers are in good agreement with those obtained in optical preforms previously [19,20] and, in particular with our results, those reported in [15], where the refractivity of  $\text{P}_2\text{O}_5$  was found to be  $0.88 \times 10^{-3}$  (compared to  $0.9 \times 10^{-3}$  from Equation (1)) and the refractivity of  $\text{Al}_2\text{O}_3$  was found to be  $2.5 \times 10^{-3}$  (compared to  $2.2 \times 10^{-3}$  from Equation (2)).

As was mentioned above, the refractive index of the PAS glass is defined mainly by the difference in concentration of  $\text{P}_2\text{O}_5$  and  $\text{Al}_2\text{O}_3$ . This difference exactly corresponds to the concentration of the excess dopant, which is incorporated into silica glass in its ordinary form ( $\text{P}_2\text{O}_5$  or  $\text{Al}_2\text{O}_3$ ). To obtain this concentration, we calculated the formal concentration of  $\text{P}_2\text{O}_5$  and  $\text{Al}_2\text{O}_3$  (without taking into consideration the formation of the  $\text{AlPO}_4$  joint),

then subtracted  $C(\text{P}_2\text{O}_5)$  from  $C(\text{Al}_2\text{O}_3)$ , which provided us with the value of concentration mismatch  $\Delta C$ :

$$\Delta C = C(\text{Al}_2\text{O}_3) - C(\text{P}_2\text{O}_5) \tag{3}$$

The positive result of such a subtraction ( $\Delta C > 0$ ) corresponds to the case of Al-excess and negative ( $\Delta C < 0$ ) to the case of P-excess. The absolute value of  $\Delta C$  corresponds to the concentration of dopant in excess ( $\text{P}_2\text{O}_5$  or  $\text{Al}_2\text{O}_3$ ).

The results of the measurements of RIP and the compound in fibers simultaneously doped with phosphorous and aluminum are presented in Figure 4, where the dependence of  $\Delta n$  (the difference between the refractive index of the PAS glass and undoped silica glass) was plotted as a function of concentration mismatch ( $\Delta C$ ) at the same point of the fiber under study. The distribution of dopants in many fiber samples was not uniform (similar to the fiber PAS#2 shown in Figure 2), which allowed us to use one to three positions along the radius for data collection. As the concentration of the  $\text{AlPO}_4$  joint may also affect the refractive index difference, we drew points corresponding to different net concentrations of  $\text{AlPO}_4$  with different symbols and colors (we chose three concentration ranges—see Figure 4).

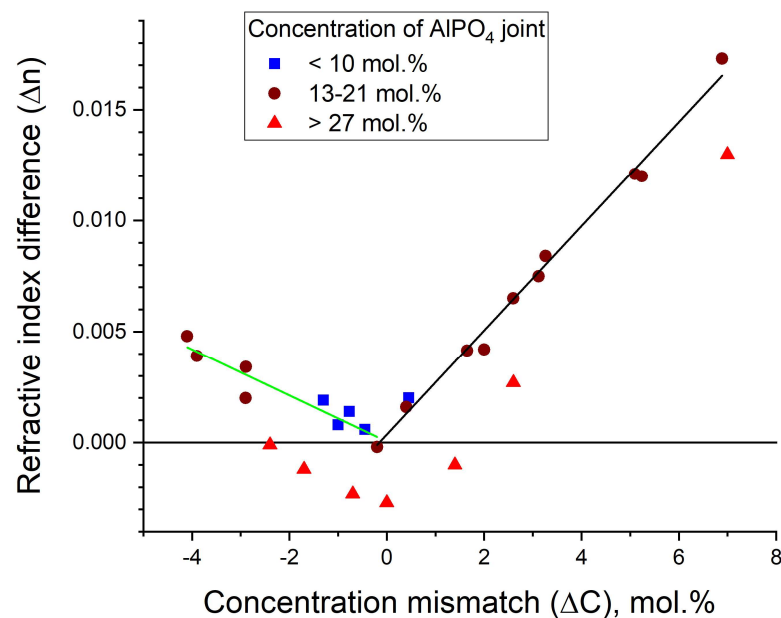


**Figure 4.** Dependence of refractive index difference between core and undoped silica glass cladding on concentration mismatch between  $\text{Al}_2\text{O}_3$  and  $\text{P}_2\text{O}_5$  for different concentrations of  $\text{AlPO}_4$  joint.

It can be seen that for fibers with a concentration of the  $\text{AlPO}_4$  joint below 21 mol.% the main trend is quite clear. In the region of phosphorous excess, the refractive index grows with the increase in the difference between the concentration of  $\text{P}_2\text{O}_5$  and  $\text{Al}_2\text{O}_3$ . Similar behavior was observed in the region of aluminum excess (but, in this case, the refractive index growth was used with the increase in the difference between the concentration of  $\text{Al}_2\text{O}_3$  and  $\text{P}_2\text{O}_5$ ) with linear approximation for regions where  $\Delta C < 0$  and for regions where  $\Delta C > 0$ , as shown in the following equation:

$$\Delta n = (0.05 \pm 0.3) \times 10^{-3} + (1.04 \pm 0.14) \times 10^{-3} \times |\Delta C|, \text{ for } \Delta C < 0 \tag{4}$$

$$\Delta n = (0.35 \pm 0.26) \times 10^{-3} + (2.35 \pm 0.07) \times 10^{-3} \times |\Delta C|, \text{ for } \Delta C > 0 \tag{5}$$

where  $\Delta C$  is given in mol.%.

In each equation, the first term shows the constant component related to  $\text{AlPO}_4$  refractivity, which is close to zero within the accuracy of the measurements ( $3 \times 10^{-4}$ ). The second term shows the refractivity of an excess amount of  $\text{P}_2\text{O}_5$  (Equation (4)) and  $\text{Al}_2\text{O}_3$

(Equation (5)). For fibers with a concentration of  $\text{AlPO}_4 > 27 \text{ mol.}\%$ , the dependence looks similar (growing with an increase in  $\Delta C$  and a similar slope), but all the points are shifted down by  $\sim 0.003\text{--}0.004$ .

In general, it is quite natural to suggest that the refractivity of excess amounts of  $\text{P}_2\text{O}_5$  and  $\text{Al}_2\text{O}_3$  remains the same independently of the concentration of  $\text{AlPO}_4$ . Such a suggestion allows us to reveal the refractivity of the  $\text{AlPO}_4$  joint by itself. For this aim, we used the data from Figure 4 but calculated the refractivity of  $\text{AlPO}_4$  ( $\Delta n_{\text{AlPO}_4}$ ) using the following formula:

$$\Delta n_{\text{AlPO}_4} = \Delta n - 1.04 \times 10^{-3} \times |\Delta C|, \text{ for } \Delta C < 0 \tag{6}$$

$$\Delta n_{\text{AlPO}_4} = \Delta n - 2.35 \times 10^{-3} \times |\Delta C|, \text{ for } \Delta C > 0 \tag{7}$$

In Figure 5, the obtained data are shown as the dependence of the  $\text{AlPO}_4$  concentration.

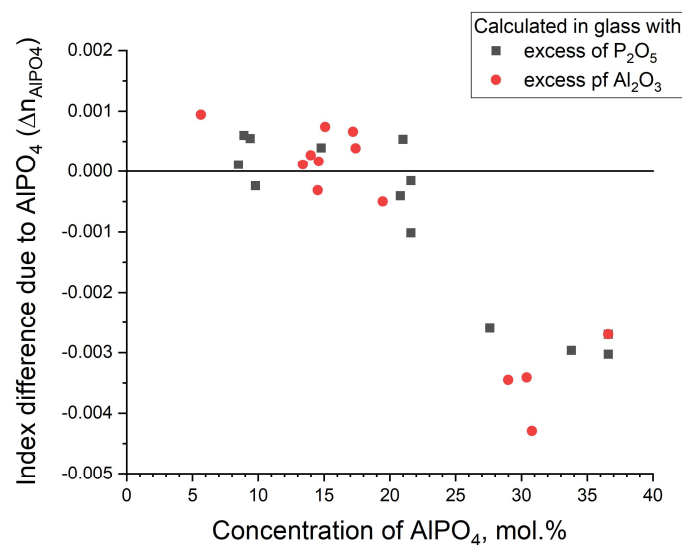


Figure 5. Dependence of refractive index difference caused by  $\text{AlPO}_4$  joint depending on its concentration.

#### 4. Discussion

Our study reveals that PAS fiber exhibits a significant (for LMA fibers) change in the refractive index profile compared to that in preforms, which must be taken into account. An analysis of sets of fibers with different levels of doping with aluminum and phosphorous allowed us to reveal the dependence of the refractive index on the concentration of the dopants. First, it should be noted that the main tendency observed earlier in preforms remains valid; the strongest effect, which defines the refractive index of PAS glass, is the formation of the  $\text{AlPO}_4$  joint. Thus, the resulting refractive index of the core depends on the refractivity of the  $\text{AlPO}_4$  joint and the refractivity of the dopant being in excess (aluminum or phosphorous); however, in the last case, only an excess concentration  $|\Delta C|$  impacted the refractive index profile.

It is quite interesting that the current study reveals the refractivity of both  $\text{Al}_2\text{O}_3$  and  $\text{P}_2\text{O}_5$  remains the same (within measurements of error) for PAS glass and for binary glasses (aluminosilicate and phosphorosilicate). Moreover, the obtained values of  $\text{Al}_2\text{O}_3$  and  $\text{P}_2\text{O}_5$  refractivity (Formulars (1), (2), (4) and (5)) are quite similar to that measured in the preforms [15,19,20].

Thus, the main difference between the RIP in fibers and in preform is caused by the different refractivity of the  $\text{AlPO}_4$  joint in the fiber and preforms. The measurement of the preforms demonstrates that the refractive index reduces by 0.0001 for each 1 mol.% of  $\text{AlPO}_4$  [1,15]. In the fibers drawn from the same preforms, the refractivity of the  $\text{AlPO}_4$  joint is nearly zero for the concentration of  $\text{AlPO}_4$  up to 21 mol.%. Thus, after drawing

the fiber, the refractive index of the core increases by 0.0001 for each mol.% of the  $\text{AlPO}_4$  joint (the difference in the refractivity of the  $\text{AlPO}_4$  joint in fibers and in preforms). This means that to predict the refractive index in the optical fiber, it is necessary to know the approximate concentration of  $\text{AlPO}_4$  in the core. However, the situation becomes more complex if the  $\text{AlPO}_4$  joint's concentration changes along the radius. In this case, not only would the average core refractive index increase, but also the RIP would change (as it is shown in Figure 2). In this case, exact data on the core compound or direct measurements of the fiber refractive index profile are required to predict the fiber's optical properties.

The most probable reason for this effect is the stress that appears in the core of PAS fiber due to the difference in the thermal diffusion coefficient with undoped silica cladding [1]. The thermal history in optical fiber is different from that in preform—during drawing, optical fibers exhibit nearly instantaneous cooling due to their high drawing speed, thin fiber diameter and localized heating zone. These cooling conditions are very different from the case of optical preforms—its diameter is typically two orders in magnitude larger, and the cooling rate due to this reason is two times smaller. As a result, stress generates different index changes in the optical fibers and fiber preforms. One possible reason for the refractive index increase might be the non-complete formation of the  $\text{AlPO}_4$  joint [16], though previously, it was observed only for low dopant concentrations, so we suggest that it is not the main factor responsible for the observed refractive index increase.

It is also interesting that for the  $\text{AlPO}_4$  joint's concentration in an excess of 27 mol.%, the behavior of the core refractive index changes completely. In this case, doping with the  $\text{AlPO}_4$  joint reduces the refractive index of the core by 0.003–0.004 compared to undoped silica glass. It is quite similar to the refractive index change observed early in bulk glass and preforms [1,15]. It must be noted that such a concentration is quite close to the critical one when the phase separation in  $\text{SiO}_2$ - $\text{AlPO}_4$  glass is suggested [15]. In some of these samples, the scanned electron microscope image in Z-contrast (BSE) gives clear evidence of this process. An example is presented in Figure 6, where the strong non-uniformity of the core was observed, indicating phase separation. We suggest that in this case, micro- or nano- $\text{AlPO}_4$ -rich clusters and cristobalite appear, and a similar process was observed earlier in highly Yb-doped PAS glasses [21], while the presence of cristobalite was confirmed via the measurements of the X-ray pattern of the preform core. An observed devitrification might change the behavior of the glass. In particular, stresses inside the core caused by such phase separation might be a reason for the core refractive index reduction. Typically, when such phase separation in the fiber core occurs, the optical losses increase to the levels of units and even tens dB/m, making such fiber useless for practice.

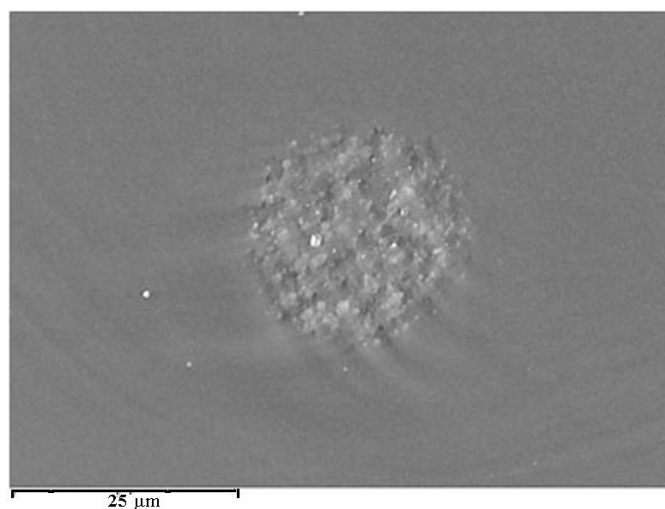


**Figure 6.** Scanned electron microscope image in Z-contrast (BSE) of the fiber core doped with 27.6 mol.% of  $\text{AlPO}_4$ .

It is also very important that the observed refractive index change limits the minimum core numerical aperture, which could be achieved. In particular, this becomes critical in highly Yb-doped optical fibers, where the additional refractivity of the  $\text{Yb}_2\text{O}_3$  can further increase the core-cladding refractive index difference. A possible solution to this problem could be the fabrication of the Ge-doped pedestal around the core, which reduces the core/first cladding refractive index difference. Moreover, an increase in the radius of such a pedestal and the removal of pure-silica glass (similar to [12]) could allow a strictly single mode of LMA optical fibers to be created that is very high Yb-doped. At the same time, knowledge of the core compound becomes very important in fibers with a pedestal. As can be seen from Figure 2, after drawing, the fiber refractive index's change behavior is different for germanosilicate and PAS glass. Fiber RIP (mainly core/first cladding numerical aperture) changes significantly compared to that in the preform.

In conclusion, for LMA PAS fibers, it becomes very important to know the concentration of dopants and their distribution along the core to predict RIP in the optical fiber. As was demonstrated in our study, a significant change in RIP after drawing the preform of the optical fibers can be observed. The most probable reason for refractive index change is mechanical stress inside the core, which can be different in optical fibers and preforms due to different cooling conditions.

**Author Contributions:** Conceptualization, M.E.L. and M.M.B.; methodology, M.E.L., S.S.A. and L.D.I.; validation, T.S.Z., V.A.A. and L.D.I.; formal analysis, M.E.L.; investigation, T.S.Z., V.A.A., L.D.I., A.S.L. and D.S.L.; resources, M.E.L., A.S.L. and D.S.L.; data curation, M.E.L. and L.D.I.; writing—original draft preparation, M.E.L.; writing—review and editing, M.E.L., L.D.I., S.S.A. and D.S.L.; visualization, M.E.L.; supervision, M.E.L., M.M.B. and D.S.L.; project administration, M.E.L.; funding acquisition, M.E.L. All authors have read and agreed to the published version of the manuscript.

**Funding:** This work was supported by the Center of Excellence “Center of Photonics” funded by the Ministry of Science and Higher Education of the Russian Federation under Contract 075-15-2022-315.

**Institutional Review Board Statement:** Not applicable.

**Informed Consent Statement:** Not applicable.

**Data Availability Statement:** The data are contained within the article.

**Acknowledgments:** The authors thank the staff of the Large-scale research facilities “Fibers” (UNU Fibers) of GPI RAS for their help with the fabrication and characterization of the used fibers.

**Conflicts of Interest:** The authors declare no conflict of interest.

## References

1. DiGiovanni, D.J.; MacChesney, J.B.; Kometani, T.Y. Structure and Properties of Silica Containing Aluminum and Phosphorus near the  $\text{AlPO}_4$  Join. *J. Non-Cryst. Solids* **1989**, *113*, 58–64. [[CrossRef](#)]
2. Unger, S.; Schwuchow, A.; Dellith, J.; Kirchhof, J. Codoped materials for high power lasers—Diffusion behavior and optical properties. *Proc. SPIE* **2007**, *6469*, 646913.
3. Kosinski, S.G.; Krol, D.M.; Duncan, T.M.; Douglass, D.C.; MacChesney, J.B.; Simpson, J.R. Raman and NMR Spectroscopy of  $\text{SiO}_2$  Glasses Co-Doped with  $\text{Al}_2\text{O}_3$  and  $\text{P}_2\text{O}_5$ . *J. Non-Cryst. Solids* **1988**, *105*, 45–52. [[CrossRef](#)]
4. Likhachev, M.E.; Bubnov, M.M.; Zotov, K.V.; Lipatov, D.S.; Yashkov, M.V.; Guryanov, A.N. Effect of the  $\text{AlPO}_4$  join on the pump-to-signal conversion efficiency in heavily Er-doped fibers. *Opt. Lett.* **2009**, *34*, 3355–3357. [[CrossRef](#)] [[PubMed](#)]
5. Suzuki, S.; McKay, H.A.; Peng, X.; Fu, L.; Dong, L.G. Highly ytterbium-doped silica fibers with low photo-darkening. *Opt. Express* **2009**, *17*, 9924–9932. [[CrossRef](#)] [[PubMed](#)]
6. Likhachev, M.; Aleshkina, S.; Shubin, A.; Bubnov, M.; Dianov, E.; Lipatov, D.; Guryanov, A. Large-Mode-Area Highly Yb-doped Photodarkening-Free  $\text{Al}_2\text{O}_3$ - $\text{P}_2\text{O}_5$ - $\text{SiO}_2$ -Based Fiber. In Proceedings of the European Conference on Lasers and Electro-Optics, Munich, Germany, 22–26 May 2011; p. CJ.P.24. [[CrossRef](#)]
7. Jetschke, S.; Unger, S.; Schwuchow, A.; Leich, M.; Kirchhof, J. Efficient Yb laser fibers with low photodarkening by optimization of the core composition. *Opt. Express* **2008**, *16*, 15540–15545. [[CrossRef](#)] [[PubMed](#)]
8. Unger, S.; Schwuchow, A.; Jetschke, S.; Reichel, V.; Leich, M.; Scheffel, A.; Kirchhof, J. Influence of aluminium-phosphorus codoping on optical properties of ytterbium-doped laser fibers. *Proc. SPIE* **2009**, *7212*, 324–332. [[CrossRef](#)]

9. Tiabi, N.; Dauliat, R.; Auguste, J.L.; Vergnole, S.; Florian, P.; Canizares, A.; Duclere, J.R.; Wondraczek, K.; Roy, P. Investigating the glass structure of Yb<sup>3+</sup>/Al<sup>3+</sup>/P<sup>5+</sup> doped silica preforms prepared by suspension method. *Opt. Mater. Express* **2023**, *13*, 3309–3319. [[CrossRef](#)]
10. Zhai, Z.; Sahu, J.K. 1480 nm Diode-Pumped Er<sup>3+</sup>:Yb<sup>3+</sup> Co-Doped Phospho-Alumino-Silicate Fiber for Extending the L-Band Gain Up to 1625 nm. *J. Light. Technol.* **2023**, *41*, 3432–3437. [[CrossRef](#)]
11. Wang, F.; Hu, L.; Xu, W.; Wang, M.; Feng, S.; Ren, J.; Zhang, L.; Chen, D.; Ollier, N.; Gao, G.; et al. Manipulating refractive index, homogeneity and spectroscopy of Yb<sup>3+</sup>-doped silica-core glass towards high-power large mode area photonic crystal fiber lasers. *Opt. Express* **2017**, *25*, 25960–25969. [[CrossRef](#)] [[PubMed](#)]
12. Sidharthan, R.; Lin, D.; Lim, K.J.; Li, H.; Lim, S.H.; Richardson, D.J.; Yoo, S. Ultra-low NA step-index large mode area Yb-doped fiber with a germanium doped cladding for high power pulse amplification. *Opt. Lett.* **2020**, *45*, 3828–3831. [[CrossRef](#)] [[PubMed](#)]
13. Wang, Z.; Zhan, H.; Ni, L.; Peng, K.; Wang, X.; Wang, J.; Jing, F.; Lin, A. Research progress of chelate precursor doping method to fabricate Yb-doped large-mode-area silica fibers for kW-level laser. *Laser Phys.* **2015**, *25*, 115103. [[CrossRef](#)]
14. Kong, F.; Dunn, C.; Parsons, J.; Kalichevsky-Dong, M.T.; Hawkins, T.W.; Jones, M.; Dong, L. Large-mode-area fibers operating near single-mode regime. *Opt. Express* **2016**, *24*, 10295–10301. [[CrossRef](#)] [[PubMed](#)]
15. Bubnov, M.M.; Guryanov, A.N.; Zotov, K.V.; Iskhakova, L.D.; Lavrishev, S.V.; Lipatov, D.S.; Likhachev, M.E.; Rybaltovskiy, A.A.; Khopin, V.F.; Yashkov, M.V.; et al. Properties of fibers with phosphoaluminosilica core. *Quantum Electron.* **2009**, *39*, 857–862. [[CrossRef](#)]
16. Kuhn, S.; Hein, S.; Hupel, C.; Nold, J.; Haarlammert, N.; Schreiber, T.; Eberhardt, R.; Tünnermann, A. Modelling the refractive index behavior of Al,P-doped SiO<sub>2</sub>, fabricated by means of all-solution doping, in the vicinity of Al:P = 1:1. *Opt. Mater. Express* **2018**, *8*, 1328–1340. [[CrossRef](#)]
17. Available online: [https://coherentinc.my.site.com/Coherent/specialty-optical-fibers/LMA-YDF-30\\_250-HI-M\\_PLUS?cclcl=en\\_US](https://coherentinc.my.site.com/Coherent/specialty-optical-fibers/LMA-YDF-30_250-HI-M_PLUS?cclcl=en_US) (accessed on 22 November 2023).
18. Yablon, A.D.; Yan, M.F.; DiGiovanni, D.J.; Lines, M.E.; Jones, S.L.; Ridgway, D.N.; Sandels, G.A.; White, I.A.; Wisk, P.; Di-Marcello, F.V.; et al. Frozen-In Viscoelasticity for Novel Beam Expanders and High-Power Connectors. *J. Light. Technol.* **2004**, *22*, 16–23. [[CrossRef](#)]
19. Bubnov, M.M.; Dianov, E.M.; Egorova, O.N.; Semjonov, S.L.; Guryanov, A.N.; Khopin, V.F.; DeLiso, E.M. Fabrication and investigation of single-mode highly phosphorus-doped fibers for Raman lasers. *Proc. SPIE* **2000**, *4083*, 12. [[CrossRef](#)]
20. Shigeo, A.; Roy, R. Revised phase diagram for the system Al<sub>2</sub>O<sub>3</sub>—SiO<sub>2</sub>. *J. Am. Ceram. Soc.* **1962**, *45*, 229–242. [[CrossRef](#)]
21. Iskhakova, L.D.; Milovich, F.O.; Likhachev, M.E.; Lipatov, D.S.; Yashkov, M.V.; Lobanov, A.S.; Guryanov, A.N. Analysis of elemental distributions and phase separation in rare-earth-doped silica-based fiber preforms and optical fibers. *J. Non-Cryst. Solids* **2021**, *554*, 120616. [[CrossRef](#)]

**Disclaimer/Publisher’s Note:** The statements, opinions and data contained in all publications are solely those of the individual author(s) and contributor(s) and not of MDPI and/or the editor(s). MDPI and/or the editor(s) disclaim responsibility for any injury to people or property resulting from any ideas, methods, instructions or products referred to in the content.